

Luminescent Cell-Penetrating Pentadecanuclear Lanthanide Clusters

Dominique T. Thielemann,[†] Anna T. Wagner,[†] Esther Rösch,[‡] Dominik K. Kölmel,[‡] Joachim G. Heck,[†] Birgit Rudat,[‡] Marco Neumaier,[†] Claus Feldmann,[†] Ute Schepers,^{*,§} Stefan Bräse,^{*,‡,§} and Peter W. Roesky^{*,†}

[†]Institute of Inorganic Chemistry and [‡]Institute of Organic Chemistry, Karlsruhe Institute of Technology, 76131 Karlsruhe, Germany

[§]Institute of Toxicology and Genetics, Karlsruhe Institute of Technology, 76344 Eggenstein-Leopoldshafen, Germany

S Supporting Information

ABSTRACT: A novel pentadecanuclear lanthanide hydroxy cluster $[\{Ln_{15}(\mu_3-OH)_{20}(PepCO_2)_{10}(DBM)_{10}Cl\}-Cl_4]$ ($Ln = Eu$ (**1**), Tb (**2**)) featuring the first example with peptoids as supporting ligands was prepared and fully characterized. The solid-state structures of **1** and **2** were established via single-crystal X-ray crystallography. ESI-MS experiments revealed the retention of the cluster core in solution. Although OH groups are present, **1** showed intense red fluorescence with 11(1)% absolute quantum yield, whereas the emission intensity and the quantum yield of **2** were significantly weaker. *In vitro* investigations on **1** and **2** with HeLa tumor cells revealed an accumulation of the clusters in the endosomal–lysosomal system, as confirmed by confocal microscopy in the TRLLM mode. The cytotoxicity of **1** and **2** toward the HeLa cells is moderate.

Luminescent materials were used in past decades in cell biology and biochemistry to get a better understanding of the structure and function of biological systems through methods that involve minimal perturbation of the system. As luminescent materials, organic fluorophores,¹ recombinant proteins,² semiconductor nanoparticles,³ and emissive metal complexes were used.⁴ The drawback of organic dyes is that they are not stable against bleaching, have a poor extinction coefficient or quantum yield, and are sometimes toxic to cells. Regarding nanoparticles and emissive metal complexes, rare-earth metal-based materials have been studied intensively because trivalent rare-earth metal ions have useful properties as optical probes,⁵ since the *f*–*f* emission lines of Pr(III), Sm(III), Eu(III), Tb(III), Dy(III), and Tm(III) ions are in the visible range.⁶ Moreover, the emission lines of the rare-earth metals are sharp because the excitation of an electron into a 4*f* orbital of higher energy is almost not influenced by the ligands in a metal complex. Most work that has been published in the area of luminescent rare-earth metal complexes deals with Eu(III) and Tb(III) because the excited states of these ions are less sensitive to vibrational quenching by intra- or intermolecular energy transfer to adjacent high-energy vibrators such as hydroxyl groups.⁷ The advantage of using mononuclear rare-earth metal complexes as cellular probes in general is their rational design.^{4,8} However, the susceptibility of rare-earth metal and in particular lanthanide(III) (Ln(III)) ion luminescence to quenching effects caused by water or hydroxyl groups is a drawback of such mononuclear complexes.⁹ Besides

mononuclear complexes, semiconductor nanoparticles such as quantum dots (QDs) have attracted a number of researchers, since their luminescence is not as prone to quenching effects as is the case for Ln metal complexes. QDs show characteristic size- and composition-dependent luminescence which can be tuned precisely.¹⁰ The third class of compounds that has been proposed as optical markers are rare-earth metal-based nanoparticles.¹¹ In comparison to QDs, they have a much longer fluorescence lifetime, and the fluorescence wavelength of Ln(III) ions is not sensitive to particle size.¹¹

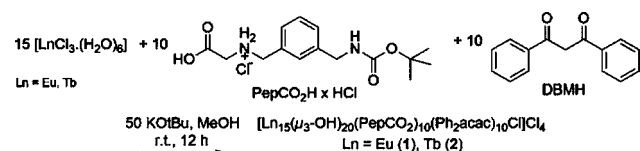
Obviously there is a large gap in size between well-defined mononuclear lanthanide complexes and polynuclear nanoparticles. The size of the latter can only be controlled within a certain range, resulting in a particle size distribution instead of defined structures. Between these two extremes, oligonuclear lanthanide clusters are accommodated. Such cluster compounds are much larger than mononuclear compounds but still exhibit a well-defined size and composition.¹² As a result of these properties, the study of the function and properties of these compounds is simplified when compared with that of nanoparticles. Today a range of lanthanide hydroxy clusters exhibiting various nuclearities has been established, highlighting the ease of preparation and good yields.¹² Although some of these compounds were studied in terms of their magnetic properties,¹³ the photophysical properties of only very few lanthanide hydroxy clusters were investigated.¹⁴ To the best of our knowledge, oligonuclear clusters of the rare-earth metals have hitherto not been used for any biological application. Based on this consideration, we were interested in synthesizing rare-earth metal-based clusters having luminescent properties for living cell penetration. To reach this goal, the anchoring of a cell-penetrating agent onto a structurally well-defined rare-earth metal cluster is necessary. Recently, Schiff-base-ligated hexanuclear zinc macrocycles were evaluated against several cell lines with respect to their toxicity, providing an example of metal clusters being investigated with regard to their potential as anti-tumor drugs or cellular localization probes.¹⁵

In 1994, the intrinsic cell-penetrating peptide (CPP) research began with the identification of the polycationic homeoprotein *Antennapedia* from *Drosophila melanogaster*.¹⁶ The currently used CPPs consist of 10–30 α -amino acids. It was shown that they can carry cargos into the cell-like peptides and proteins up to 120 kDa—oligonucleotides,¹⁷ liposomes,¹⁸ and nanoparticles.¹⁹ The

Received: April 9, 2013

Published: May 7, 2013



Scheme 1. Synthesis of Eu and Tb Clusters **1** and **2**^a

^aKeto–enol tautomerization of DBMH is omitted for clarity.

fast cellular uptake and the defined structure make CPPs very attractive, but their applicability is also restricted since they are prone to enzymatic degradation. To circumvent the latter aspect, peptidomimetics such as cell-penetrating peptoids (CPPos) are increasingly used.²⁰ CPPos are based on oligo-*N*-alkylglycine varying in different side chains connected to the *N*-atom of the backbone. Peptoids are stable against proteases *in vivo* and *in vitro*, and they exhibit antibiotic properties. Furthermore, they possess a binding affinity to certain receptors or proteins.^{20d}

Herein we report on pentadecanuclear europium and terbium hydroxy clusters which are ligated by CPPo monomers. Owing to the distinct biological compatibility of the peptoids, the obtained clusters feature a pronounced propensity to cell penetration. Reaction of the CPPo monomer 2-[[3-(((*tert*-butoxycarbonyl)amino)methyl)benzyl]amino]acetic acid hydrochloride (PepCO₂H·HCl) with [LnCl₃·(H₂O)₆] (Ln = Eu, Tb) and dibenzoylmethane (DBMH) in the presence of potassium *tert*-butoxide in methanol resulted in the formation of the pentadecanuclear lanthanide hydroxy cluster [Ln₁₅(μ₃-OH)₂₀(PepCO₂)₁₀(DBM)₁₀Cl]Cl₄ (Ln = Eu (**1**), Tb (**2**)) in 40% (**1**) and 33% (**2**) single-crystalline yield, respectively (Scheme 1).

Compounds **1** and **2** were characterized by standard analytical and spectroscopic techniques (Supporting Information). The solid-state structures were determined by single-crystal X-ray diffraction (Figure 1). Although the X-ray data collected from **1** were very poor, its composition was deduced. The composition was also established by ESI-MS (see below). The [Ln₁₅(μ₃-OH)₂₀(PepCO₂)₁₀(DBM)₁₀Cl]⁴⁺ cation consists of five {Ln₄(μ₃-OH)₄}⁸⁺ heterocubane subunits, which are fused to a pentagonal ring structure by an edge-sharing arrangement. The cyclic shape of this metal hydroxide scaffold is additionally stabilized by a centered μ₅-bridging Cl-atom. The 10 dibenzoylmethanide (DBM) ligands are bidentate and coordinate uniformly in a chelating κ²-mode to those rare-earth metal atoms which do not act as linking points between adjacent heterocubane subunits. All DBM ligands are aligned coplanar with the pentagonal ring. In contrast, the CPPo monomer (PepCO₂) ligands act exclusively as tridentate ligands and are arranged perpendicular to the ring. Each PepCO₂ ligand coordinates with both carboxylate O-atoms and the glycinic N-atom to three metal centers, giving a μ₃:κ²:κ¹-mode. Although a similar central structural core of formula {Ln₁₅(μ₃-OH)₂₀Cl}²⁴⁺ has been reported,²¹ coordination of CPPo monomers to such an inorganic core structure is, to the best of our knowledge, unique.

Although numerous rare-earth metal hydroxy clusters can be found in literature,¹² almost nothing is known about their structure in solution.²² To investigate the stability in solution, ESI-MS spectra of **1** and **2** were recorded from different solvents. For all compounds the [{Ln₁₅(μ₃-OH)₂₀(PepCO₂)₁₀(DBM)₁₀-Cl]Cl₂}²⁺ (M₀²⁺) cation could be unambiguously detected from various alcoholic solvents (Figures 2, S4, and S5) and DMF; i.e., in the chosen medium the dissolution process of **1** is accompanied by the dissociation of two non-coordinating

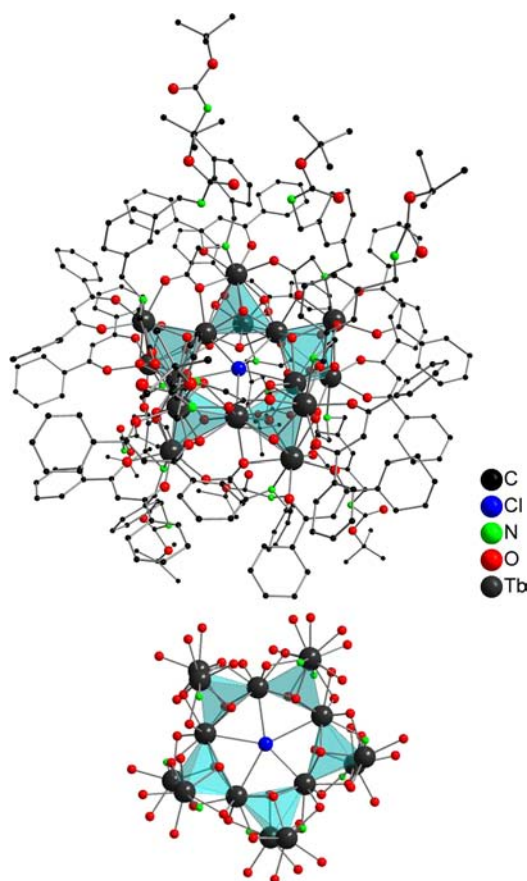


Figure 1. Top: Front view of solid-state structure of [Tb₁₅(μ₃-OH)₂₀(PepCO₂)₁₀(DBM)₁₀Cl]Cl₄ (**2**). Bottom: view of the inorganic {Tb₁₅(μ₃-OH)₂₀Cl}²⁴⁺ core with all ligand-derived coordinating heteroatoms. H-atoms are omitted for clarity.

chloride anions. Figures 2 and S5 show cutouts of the ESI-MS spectra of **1** and **2** from ethanol solution, and the insets highlight the agreement between calculated and experimentally found *m/z* ratio as well as the expected isotopic distribution of the dication M₀²⁺. As can be seen from Figures 2 and S4, adjacent signal sets with identical isotopic distribution shifted to higher *m/z* ratios are indicative of an exchange reaction, which is attributed to substitution of hydroxy bridges by ethanol-derived ethoxy groups. Upon this exchange process, the cluster scaffold is retained, as illustrated by the corresponding sum formula [{Ln₁₅(μ₃-OH)_{20-n}(OEt)_n(PepCO₂)₁₀(DBM)₁₀Cl]Cl₂}²⁺ (M_n²⁺) with *n* = 1–3, showing that 1–3 hydroxy bridges are substituted in M₀²⁺. These degradation processes were found to occur consecutively (for **1**, refer to Figure S4).

Compound **1** showed intense red fluorescence with the characteristic Eu³⁺-related *f*→*f* transitions at 580–700 nm (Figure 3). Considering the direct coordination of the luminescent center to hydroxide anions, the quantum yield at room temperature is surprisingly high. Thus, values of 19(1)% relative to YVO₄:Eu (λ_{exc.} = 365 nm) as a reference and of 16(1)% (λ_{exc.} = 400 nm) for absolute counting of photons were obtained (cf. Supporting Information). Most often the emission of rare-earth ions is quenched via vibronic transitions in the presence of hydroxyl or aqua ligands.²³ Compound **2** showed typical *f*→*f* emission lines of Tb³⁺ (550–650 nm). In comparison to **1**, the emission intensity and the quantum yield (<3%) are, however, significantly weaker (Figure S6).

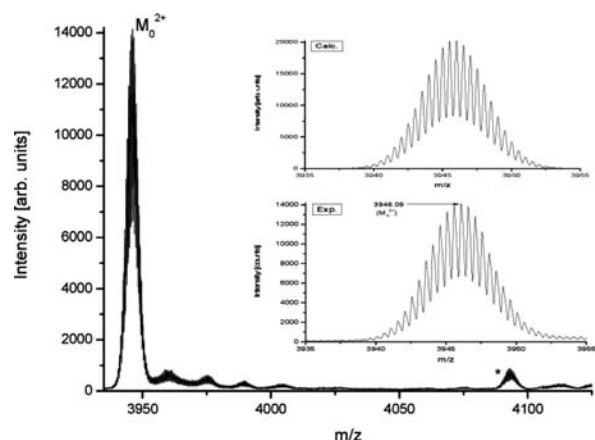


Figure 2. Cationic electrospray (ESI⁺) spectrum of **1** from ethanol. The ion signal for M_0^{2+} at $m/z = 3946.09$ can clearly be assigned to the dicationic species $[\{\text{Eu}_{15}(\mu_3\text{-OH})_{20}(\text{PepCO}_2)_{10}(\text{DBM})_{10}\text{Cl}\}_2\text{Cl}_2]^{2+}$. Peaks marked with an asterisk are due to adduct formation through a PepCO_2H ligand (either from solution or due to the electrospray process). Inset: Comparison of the calculated (top) and measured (bottom) isotopic distribution of M_0^{2+} .

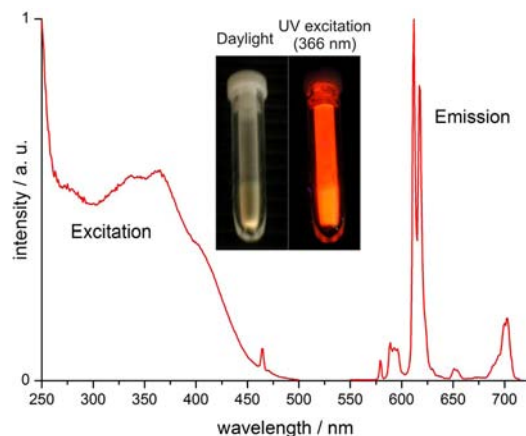


Figure 3. Excitation/emission spectra of **1** and photograph of the compound in daylight and under 366 nm excitation.

To date, luminescent lanthanide complexes are increasingly being used as luminescent labels for bioimaging²⁴ as well as for simultaneous labeling of biological structures in electron microscopy or magnetic resonance imaging (MRI).²⁵ Europium and terbium clusters **1** and **2** were tested for their applicability as luminescent probes in cell culture. To monitor their cellular uptake and the intracellular routing, we used conventional fluorescent confocal microscopy and time-resolved long-lived luminescent microscopy (TRLLM), which is capable of gating out the undesirable cell-derived short-lived luminescence.²⁶ Although there are many publications on luminescent lanthanide complexes, only a few of them have yet been used for luminescence microscopy via TRLLM, since the imaging requires kinetic stability in water and a so-called sensitizing unit that generates an efficient antenna effect.²⁶ To determine a suitable working concentration in cell culture, a MTT viability assay was performed (Figure S7). The clusters are moderately toxic, with $\text{LD}_{50} = 13.62 \mu\text{M}$ for **1** and $4.61 \mu\text{M}$ for **2** in human cervical carcinoma (HeLa) cells. Eventually, **1** and **2** were applied in cell culture experiments at $0.1\text{--}1 \mu\text{M}$ concentration using HeLa cells. By gating out the short-lived autofluorescence from

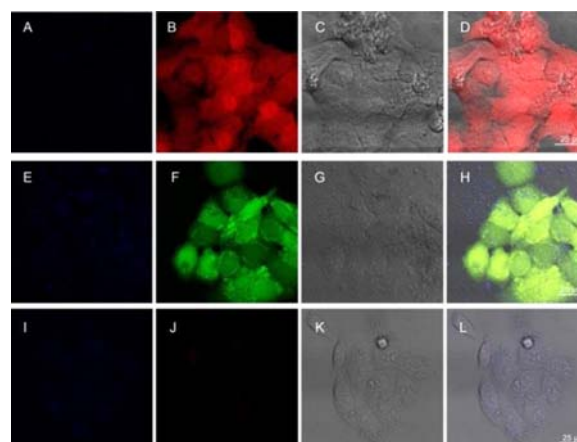


Figure 4. Cellular uptake of **1** and **2** in HeLa cells: 1×10^4 HeLa wt cells were treated with $0.1 \mu\text{M}$ **1** (A–D), **2** (E–H), or $[\text{TbCl}_3 \cdot (\text{H}_2\text{O})_6]$ (I–L) for 24 h at 37°C . $[\text{EuCl}_3 \cdot (\text{H}_2\text{O})_6]$ showed the same result as shown in panels I–L. Eventually, the cells are analyzed with time-resolved luminescence confocal imaging. Images D, H, and L show the merging of the bright-field channel with the emission channels (A–C, E–G, and I–K, respectively) for the luminescence using the PMTs with emission of 420–480 (A,E), 480–600 (F,J), and 500–700 nm (B), and the bright-field channel (C,G,K). Due to the weak luminescence of **2**, images F and H were taken from 32 accumulated frames. Scale bar = $25 \mu\text{m}$.

the cells, the intracellular luminescence of the clusters was measured.

Cluster **1** showed a strong luminescence, while the images of **2** were taken by 32-fold frame accumulation to detect the signal due to the rather weak luminescence of **2**. Compounds **1** and **2** were distributed within the cytoplasm and the nucleus (Figure 4). Additionally, they show a strong accumulation within the endosomal–lysosomal system. This suggests an endocytotic uptake and an endosomal escape, accompanied by a subsequent distribution to the cytoplasmic and nuclear compartments (Figure 4). To elucidate whether the uptake of the lanthanide clusters is based on energy-dependent endocytic processes, cellular uptake was studied for 4 h at 4°C . Energy depletion at 4°C severely reduced the uptake, giving rise to the assumption that endocytosis was involved in the cellular uptake of clusters **1** and **2**. Further studies have to be undertaken to pinpoint the exact endocytic pathway. Using $[\text{EuCl}_3 \cdot (\text{H}_2\text{O})_6]$ and $[\text{TbCl}_3 \cdot (\text{H}_2\text{O})_6]$ instead of the cluster compounds **1** and **2** as rare-earth element sources under the same incubation conditions did not result in any uptake into the cells. To prove the uptake of the clusters within the cells, a *xyl*-scan was performed. By using confocal microscopy in the TRLLM mode, a *xyl*-scan showed main luminescence emission peaks at about 617 nm for **1** and 493, 553, and 595 nm for **2**, which were slightly shifted to higher wavelengths. This bathochromic shift can be due to aggregation within the cells or solvent issues (Figure S8). These emission peaks indicate the presence of clusters **1** and **2** in the cells' interior; i.e., the cluster molecules are not just adsorbed on the surface of the cell walls. By using a related method applying *z*-axis scanning, it was recently shown that oligonucleotide-templated silver nanoclusters enter MCF-7 human breast cancer cells.²⁷

In conclusion, a novel structurally defined CPPo monomer-ligated pentadecanuclear lanthanide hydroxy cluster of formula $[\text{Ln}_{15}(\mu_3\text{-OH})_{20}(\text{PepCO}_2)_{10}(\text{DBM})_{10}\text{Cl}]\text{Cl}_4$ (Ln = Eu (**1**), Tb (**2**)) was prepared and structurally characterized. ESI-MS of these compounds revealed the retention of the cluster core when dissolved in alcohols or DMF; however, in EtOH an exchange of

hydroxy bridges by solvent-derived ethoxy groups was observed. Although hydroxyl groups are present in **1**, it showed intense red fluorescence. In comparison, the emission intensity and the quantum yield (<3%) were, as expected, significantly weaker for **2**. Since the clusters are stable in solution, they were applied in cell culture experiments. As a result of their defined structure, an exact dosage is possible. The cellular uptake is significantly different from that of a mononuclear species. Confocal fluorescence microscopy and TRILM of HeLa tumor cells treated with **1** and **2** revealed a successful internalization into the endosomes, the cytoplasm, and the nucleus. To the best of our knowledge, there has been no previous description of a similar experiment with well-defined rare-earth element clusters. Although we do not know whether the clusters are chemically modified upon the cellular uptake, the concept of using structurally well-defined clusters as optical markers was proven. The nanoscale bioaccessible clusters hold promise for potential future applications as biomarkers, especially in combined electron microscopy and fluorescence imaging as well as for MRI purposes.

■ ASSOCIATED CONTENT

● Supporting Information

Synthesis and characterization; luminescence data, $\chi\lambda$ -scans, and viability assay; full citation for ref 20c. This material is available free of charge via the Internet at <http://pubs.acs.org>.

■ AUTHOR INFORMATION

Corresponding Author

roesky@kit.edu

Notes

The authors declare no competing financial interest.

■ ACKNOWLEDGMENTS

We acknowledge the financial support provided by the Deutsche Forschungsgemeinschaft (DFG) and the DFG-Center for Functional Nanostructures (CFN) within Research Area C. The German Business Foundation (SDW) (fellowship for E.R.), the Fonds der Chemischen Industrie (fellowship to D.K.K.), and the Karlsruhe School of Optics & Photonics (KSOP) (fellowship to D.K.K. and B.R.) are acknowledged.

■ REFERENCES

- (1) Domaille, D. W.; Que, E. L.; Chang, C. J. *Nat. Chem. Biol.* **2008**, *4*, 168.
- (2) Shaner, N. C.; Steinbach, P. A.; Tsien, R. Y. *Nat. Methods* **2005**, *2*, 905.
- (3) Weng, J.; Ren, J. *Curr. Med. Chem.* **2006**, *13*, 897.
- (4) Montgomery, C. P.; Murray, B. S.; New, E. J.; Pal, R.; Parker, D. *Acc. Chem. Res.* **2009**, *42*, 925.
- (5) Eliseeva, S. V.; Bünzli, J.-C. G. *Chem. Soc. Rev.* **2010**, *39*, 189.
- (6) *Basics of Lanthanide Photophysics*; Bünzli, J.-C. G., Eliseeva, S. V., Eds.; Springer Verlag: Berlin, 2010.
- (7) (a) Dickens, R. S.; Parker, D.; Bruce, J. I.; Tozer, D. J. *Dalton Trans.* **2003**, 1264. (b) Xu, J.; Corneille, T. M.; Moore, E. G.; Law, G.-L.; Butlin, N. G.; Raymond, K. N. *J. Am. Chem. Soc.* **2011**, *133*, 19900. (c) Law, G.-L.; Pham, T. A.; Xu, J.; Raymond, K. N. *Angew. Chem.* **2012**, *124*, 2421.
- (8) Stasiuk, G. J.; Tamang, S.; Imbert, D.; Poillot, C.; Giardiello, M.; Tisseyre, C.; Barbier, E. L.; Fries, P. H.; de Waard, M.; Reiss, P.; Mazzanti, M. *ACS Nano* **2011**, *5*, 8193.
- (9) Beeby, A.; Clarkson, I. M.; Dickens, R. S.; Faulkner, S.; Parker, D.; Royle, L.; de Sousa, A. S.; Gareth Williams, J. A.; Woods, M. J. *Chem. Soc., Perkin Trans.* **1999**, *2*, 493.
- (10) Michalet, X.; Pinaud, F. F.; Bentolila, L. A.; Tsay, J. M.; Doose, S.; Li, J. J.; Sundaresan, G.; Wu, A. M.; Gambhir, S. S.; Weiss, S. *Science* **2005**, *307*, 538.
- (11) Shen, J.; Sun, L.-D.; Yan, C.-H. *Dalton Trans.* **2008**, 5687.
- (12) (a) Wang, R.; Selby, H. D.; Liu, H.; Carducci, M. D.; Jin, T.; Zheng, Z.; Anthis, J. W.; Staples, R. J. *Inorg. Chem.* **2002**, *41*, 278. (b) Zheng, Z. *Chem. Commun.* **2001**, 2521. (c) Zheng, Z. In *Handbook on the Physics and Chemistry of Rare Earths Elements*; Gschneidner, K. A., Jr., Bünzli, J.-C. G., Pecharsky, V. K., Eds.; Elsevier: Amsterdam, 2010; Vol. 40, p 109. (d) Andrews, P. C.; Gee, W. J.; Junk, P. C.; Massi, M. *New J. Chem.* **2013**, *37*, 35.
- (13) (a) Jami, A. K.; Baskar, V.; Sañudo, E. C. *Inorg. Chem.* **2013**, *52*, 2432. (b) Baskar, V.; Gopal, K.; Helliwell, M.; Tuna, F.; Wernsdorfer, W.; Wippeny, R. E. P. *Dalton Trans.* **2010**, *39*, 4747. (c) Jami, A. K.; Kishore, P. V. V. N.; Baskar, V. *Polyhedron* **2009**, *28*, 2284. (d) Gamer, M. T.; Lan, Y.; Roesky, P. W.; Powell, A. K.; Clerac, R. *Inorg. Chem.* **2008**, *47*, 6581. (e) Gu, X.; Xue, D. *Inorg. Chem.* **2007**, *46*, 3212. (f) Kong, X.-J.; Wu, Y.; Long, L.-S.; Zheng, L.-S.; Zheng, Z. *J. Am. Chem. Soc.* **2009**, *131*, 6918. (g) Wu, Y.; Morton, S.; Kong, X.; Nichol, G. S.; Zheng, Z. *Dalton Trans.* **2011**, *40*, 1041. (h) Lin, P.-H.; Burchell, T. J.; Ungur, L.; Chibotaru, L. F.; Wernsdorfer, W.; Murugesu, M. *Angew. Chem., Int. Ed.* **2009**, *48*, 9489.
- (14) (a) Hauser, C. P.; Thielemann, D. T.; Adlung, M.; Wickleder, C.; Roesky, P. W.; Weiss, C. K.; Landfester, K. *Macromol. Chem. Phys.* **2011**, *212*, 286. (b) Chen, X.-Y.; Yang, X.; Holliday, B. J. *Inorg. Chem.* **2010**, *49*, 2583. (c) Andrews, P. C.; Brown, D. H.; Fraser, B. H.; Gorham, N. T.; Junk, P. C.; Massi, M.; Pierre, T. G.; St; Skelton, B. W.; Woodward, R. C. *Dalton Trans.* **2010**, *39*, 11227.
- (15) Redshaw, C.; Elsegood, M. R. J.; Frese, J. W. A.; Ashby, S.; Chao, Y.; Mueller, A. *Chem. Commun.* **2012**, *48*, 6627.
- (16) Derossi, D.; Joliot, A. H.; Chassaing, G.; Prochiantz, A. *J. Biol. Chem.* **1994**, *269*, 10444.
- (17) Astriab-Fisher, A.; Sergueev, D. S.; Fisher, M.; Shaw, B. R.; Juliano, R. L. *Biochem. Pharmacol.* **2000**, *60*, 83.
- (18) Torchilin, V. P.; Rammohan, R.; Weissig, V.; Levchenko, T. S. *Proc. Natl. Acad. Sci. U.S.A.* **2001**, *98*, 8786.
- (19) Lewin, M.; Carlesso, N.; Tung, C. H.; Tang, X. W.; Cory, D.; Scadden, D. T.; Weissleder, R. *Nat. Biotechnol.* **2000**, *18*, 410.
- (20) (a) Schröder, T.; Niemeier, N.; Afonin, S.; Ulrich, A. S.; Krug, H. F.; Bräse, S. *J. Med. Chem.* **2008**, *51*, 376. (b) Schröder, T.; Schmitz, K.; Niemeier, N.; Balaban, T. S.; Krug, H. F.; Schepers, U.; Bräse, S. *Bioconjugate Chem.* **2007**, *18*, 342. (c) Simon, R. J.; et al. *Proc. Natl. Acad. Sci. U.S.A.* **1992**, *89*, 9367. (d) Simon, R. J.; Martin, E. J.; Miller, S. M.; Zuckermann, R. N.; Blaney, J. M.; Moos, W. H. In *Techniques in Protein Chemistry V*; Crab, J. W., Ed.; Academic Press: San Diego, CA, 1994; p 533. (e) Wender, P. A.; Mitchell, D. J.; Pattabiraman, K.; Pelkey, E. T.; Steinman, L.; Rothbard, J. B. *Proc. Natl. Acad. Sci. U.S.A.* **2000**, *97*, 13003. (f) Zuckermann, R. N.; Kodadek, T. *Curr. Opin. Mol. Ther.* **2009**, *11*, 299.
- (21) Wang, R.; Zheng, Z.; Jin, T.; Staples, R. J. *Angew. Chem., Int. Ed.* **1999**, *38*, 1813.
- (22) Löble, M. W.; Casimiro, M.; Thielemann, D. T.; Oña-Burgos, P.; Fernández, I.; Roesky, P. W.; Breher, F. *Chem.—Eur. J.* **2012**, *18*, 5325.
- (23) Blasse, G.; Grabmaier, B. C. *Luminescent Materials*; Springer: Berlin, 1994.
- (24) (a) Xue, F.; Ma, Y.; Fu, L.; Hao, R.; Shao, G.; Tang, M.; Zhang, J.; Wang, Y. *Phys. Chem. Chem. Phys.* **2010**, *12*, 3195. (b) Picot, A.; D'Aleo, A.; Baldeck, P. L.; Grichine, A.; Duperray, A.; Andraud, C.; Maury, O. *J. Am. Chem. Soc.* **2008**, *130*, 1532. (c) Deiters, E.; Song, B.; Chauvin, A. S.; Vandevyver, C. D.; Gumy, F.; Bünzli, J. C. *Chem.—Eur. J.* **2009**, *15*, 885. (d) Law, G. L.; Wong, K. L.; Man, C. W.; Wong, W. T.; Tsao, S. W.; Lam, M. H.; Lam, P. K. *J. Am. Chem. Soc.* **2008**, *130*, 3714.
- (25) Bünzli, J. C.; Piguët, C. *Chem. Soc. Rev.* **2005**, *34*, 1048.
- (26) Hanaoka, K.; Kikuchi, K.; Kobayashi, S.; Nagano, T. *J. Am. Chem. Soc.* **2007**, *129*, 13502.
- (27) Li, J.; Zhong, X.; Cheng, F.; Zhang, J.-R.; Jiang, L.-P.; Zhu, J.-J. *Anal. Chem.* **2012**, *84*, 4140.